

Neutron emission associated with $\gamma\gamma \rightarrow \gamma\gamma$ scattering in UPC of heavy ions at the LHC

P. Jucha,^{1,*} M. Klusek-Gawenda,^{1,†} and A. Szczurek^{1,2,‡}

¹*Institute of Nuclear Physics PAN, ul. Radzikowskiego 152, PL-31-342 Kraków, Poland*

²*Institute of Physics, Faculty of Exact and Technical Sciences,
University of Rzeszów, ul. Pigonia 1, PL-35-310 Rzeszów, Poland*

(Dated: July 21, 2025)

We calculate cross sections for the production of different neutron classes $0n0n$, $0nXn + Xn0n$ and $XnXn$, possible to measure in Zero Degree Calorimeters (ZDCs), associated with photon-photon scattering in UPC of lead on lead. The calculations are performed for the ATLAS kinematics. Our calculations for neutron classes are tested against existing data for ρ^0 production in UPC. We get a good agreement for absolute cross section as well as very good results for fractional cross section which gives confidence to the analogous calculation for diphoton production, corresponding to $\gamma\gamma \rightarrow \gamma\gamma$ scattering. We present both absolute as well as fractional cross sections for the different neutron classes. We also show different distributions in impact parameter, photon rapidity, transverse momentum, diphoton invariant mass and photon rapidity difference. The shapes of the photon distributions depend on the neutron classes which we quantify in this paper. It would be valuable to test our predictions using the ATLAS main detector and the ATLAS ZDCs.

I. INTRODUCTION

The light-by-light scattering (LbL) is a quantal process which was “measured” only recently in ultraperipheral collisions (UPC) of heavy ions at the LHC [1–5]. Different mechanisms were considered by us in recent years [6–8]. The box mechanism was proven to be the dominant mechanism for the ATLAS and CMS kinematics. Therefore in the following we shall include only the box mechanism (with leptons and quarks) formed in a fusion of two quasi-real photons.

The photon-photon scattering in UPC can be also studied at lower diphoton masses with ALICE and LHCb detectors [9] and in a somewhat remote future with FoCal and ALICE 3 detectors [10–12]. Taking into account the detector’s acceptance, compared to the ATLAS and CMS experiments, there may be other mechanisms.

Recently we also calculated inelastic processes where photon(s) couple to individual nucleons (proton or neutron) [13]. In such processes, called by us inelastic, one or even two nuclei are excited and may emit probably a small number of neutrons. Such processes constitute a background to purely coherent processes when photons couple rather to nuclei.

In the present paper, we consider only coherent processes. In this case emission of neutrons is caused by extra photon exchanges which lead to excitation of one or both colliding nuclei. The excited nuclei typically emit one or more neutrons which are emitted in forward and backward directions due to high-energy boosts. The formalism of neutron emission in UPC was discussed in recent years [14–21]. Calculation of the emission of a given number of neutrons is more tricky and requires modeling of

the underlying nuclear processes. However, calculating the cross section for a given class of neutron emissions is simpler and more reliable. This will be discussed in the next section.

II. FORMALISM

The cross section for LbL associated with neutron emission in lead-lead UPC is calculated in equivalent photon approximation in the impact parameter space as:

$$\sigma_{PbPb \rightarrow AA+\gamma\gamma+kn+jn} = \int \frac{d\sigma_{\gamma\gamma \rightarrow \gamma\gamma}(W_{\gamma\gamma})}{dz} S^2(b) P^c(b) \times N(\omega_1, b_1) N(\omega_2, b_2) d^2b d\bar{b}_x d\bar{b}_y \frac{W_{\gamma\gamma}}{2} dW_{\gamma\gamma} dY_{\gamma\gamma} dz. \quad (1)$$

In the outgoing channel, A stands for the lead nucleus minus k or n neutrons. The impact parameter approach is very useful as here the probability $P^c(b)$ of a given neutron category c can be easily included by inserting it under the integral in Eq. (1). $S^2(b)$ is a probability that is less than 1 for $b < R_{Pb_1} + R_{Pb_2}$, and equals 1 for the $b > R_{Pb_1} + R_{Pb_2}$. The survival probability for the rapidity gap can be calculated as

$$S^2(b) = \exp(-\sigma_{NN} \cdot T_{AB}(b)). \quad (2)$$

where σ_{NN} is the inelastic nucleon-nucleon cross section. The $T_{AB}(b)$ nuclear overlap function above means the convolution integral

$$T_{AB}(b) = \int d^2s T_A(\mathbf{s}) T_B(\mathbf{b} - \mathbf{s}), \quad (3)$$

where T_A and T_B are standard nuclear matter thickness functions $T_A(\mathbf{b}) = \int \rho(\vec{r}) dz$, where $\vec{r} = (\vec{b}, z)$.

*Electronic address: Pawel.Jucha@ifj.edu.pl

†Electronic address: Mariola.Klusek@ifj.edu.pl

‡Electronic address: Antoni.Szczurek@ifj.edu.pl

The main goal of this research is to determine the contribution of the percentage of final state ($\gamma\gamma$) production associated with the emission or absence of emission for a given process. For this purpose, we introduce a probability of the neutron category $P^c(b)$. The theoretical model on the production of particle accompanied by neutron emission was discussed e.g. in [14, 15]. We define the average number of photon interactions with a nucleus as

$$m(b) = \int d\omega N(\omega, b) \sigma_{abs}(\omega), \quad (4)$$

where $\sigma_{abs}(\omega)$ is energy dependent cross section for photon absorption. The calculations use a parametrization that takes into account the description of the physical sub-processes that give input to the photoabsorption cross section, including GDR, quasi-deuteron, Δ resonance, see Ref. [17]. Now we can define quantities that form the basis of probability calculations. We assume that the sum of probabilities for the emission of at least one neutron Xn , and the absence of neutron $0n$, gives 1:

$$\begin{aligned} P^{Xn}(b) &= 1 - \exp[-m(b)], \\ P^{0n}(b) &= \exp[-m(b)]. \end{aligned} \quad (5)$$

Having fixed the auxiliary probabilities we can calculate probabilities for well-defined neutron categories: $0n0n$, $0nXn$, $Xn0n$, $XnXn$. The impact parameter dependent probabilities can be easily calculated in an almost model-independent way as:

$$\begin{aligned} P^{XnXn}(b) &= (P^{Xn}(b))^2, \\ P^{0n0n}(b) &= (P^{0n}(b))^2, \\ P^{Xn0n}(b) &= P^{Xn}(b)P^{0n}(b). \end{aligned} \quad (6)$$

The sum of the cross sections that takes into account all configurations of neutron emissions gives the total cross section.

III. RESULTS

A. Break-up probabilities

In Fig.1 we show probabilities defined in the previous section as a function of impact parameter for all neutron categories. The probabilities are normalized to fulfill the following relation:

$$P^{0n0n}(b) + P^{0nXn}(b) + P^{Xn0n}(b) + P^{XnXn}(b) = 1. \quad (7)$$

At larger b the $0n0n$ category clearly dominates, the $Xn0n$ category reaches its maximum at $b \approx 20$ fm. In contrast, at small impact parameters $\sim 2R_A$ the $XnXn$ category is the primary one. One may say that selecting

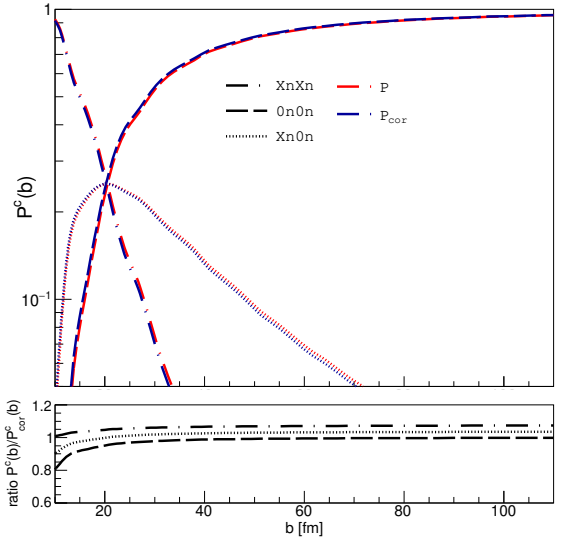


FIG. 1: Break-up probabilities as a function of impact parameter: $XnXn$ (dash-dotted line), $0n0n$ (dashed line) and $Xn0n$ (dotted line). The lower panel is explained in the main text.

a category allows to choose a characteristic impact parameter. The results presented so far are based on the assumption that absorption of photon necessarily leads to the emission of one or more neutrons. However at low excitation energies also photons can be emitted and compete with neutron emission from the excited nucleus. How important can be such an effect we know only theoretically based on statistical model codes. Recently the Experimental Storage Ring (ESR) group at GSI Darmstadt measured the competition between photon and neutron emissions. The probability of neutron emission was measured up to excitation energies $E_{exc} = 9.5$ MeV [22]. The probability increases from the threshold (neutron separation energy) and slowly converges to 1. We have parametrized the measured results of $P_n(E_{exc})$ as:

$$P_n(E_{exc}) = 1 - \exp\left[\frac{-(E_{exc} - E_{sep})}{\lambda}\right], \quad (8)$$

with $E_{sep} = 7.37$ MeV and $\lambda = 0.8$ MeV. With this correction, and $\omega = E_{exc}$ we get

$$m(b) = \int d\omega N(\omega, b) \sigma_{abs}(\omega) P_n(\omega). \quad (9)$$

The corrections on the logarithmic scale are barely visible, therefore we also show the ratio between $P^c(b)$ and $P^c_{cor}(b)$ - probability corrected by the mentioned effect, at the bottom of Fig.1.

B. Neutron emission and ρ^0 meson photoproduction

The ρ^0 production in UPC is a process which was measured at RHIC and LHC with large statistics. The cross section for the simultaneous production of ρ^0 meson in association with neutron emission can be written as

$$\sigma_{AA \rightarrow AA + \rho + kn + jn} = \int \left(\frac{dP_{\gamma\mathbb{P}}}{dy_\rho} + \frac{dP_{\mathbb{P}\gamma}}{dy_\rho} \right) \times S^2(b) P^c(b) d^2b dy_\rho, \quad (10)$$

where the rapidity-dependent probabilities are:

$$\frac{dP_{\gamma\mathbb{P}/\mathbb{P}\gamma}}{dy_\rho} = \omega_i N(\omega_i, b) \sigma(\gamma A \rightarrow \rho A; W_i) \quad (11)$$

The modeling relay therefore on calculating photoproduction cross section $\sigma(\gamma A \rightarrow \rho A; W_i)$ at phase space dependent γA energies W_i ($i = 1, 2$), $W_i^2 = 2\omega_i \sqrt{s_{NN}}$. In the following, we shall use a simple model as ρ^0 production is used only to test our approach for neutron emissions. In the vector dominance model (VDM):

$$\sigma(\gamma A \rightarrow \rho A; W_i) = \frac{d\sigma_{\gamma A \rightarrow \rho A}(W_i; t=0)}{dt} \int_{-\infty}^{t_{min}} |F_A(t)|^2 dt, \quad (12)$$

$$\sigma(\gamma A \rightarrow \rho A; W_i) = \frac{\alpha_{em}}{16\pi} \frac{4\pi}{f_\rho^2} \sigma_{tot}^2(\rho A; W_i). \quad (13)$$

In the classical mechanics Glauber approach, the total cross section for VA collisions reads:

$$\sigma_{tot}(\rho A; W_i) = \int (1 - \exp(-\sigma_{tot}(\rho p; W_i) T_A(r))) d^2r. \quad (14)$$

From the optical theorem one gets:

$$\sigma_{tot}^2(\rho p) = 16\pi \frac{d\sigma(\rho p)}{dt} \Big|_{t=0} = 16\pi \frac{f_\rho^2}{4\pi} \frac{1}{\alpha_{em}} \frac{d\sigma(\gamma p \rightarrow \rho^0 p)}{dt} \Big|_{t=0}, \quad (15)$$

We parametrize the forward ρ^0 production cross section in elementary collisions as:

$$\frac{d\sigma(\gamma p \rightarrow \rho p)}{dt} \Big|_{t=0} = B(XW_{\gamma p}^\epsilon + YW_{\gamma p}^{-\eta}). \quad (16)$$

For the ρ^0 vector meson production we take: $B = 11 \text{ GeV}^{-2}$, $X = 5 \text{ } \mu\text{b}$, $\epsilon = 0.22$, $Y = 26 \text{ } \mu\text{b}$, $\eta = 1.23$. Here for simplicity we use only one energy-independent slope parameter B , identical for Pomeron and Reggeon exchanges.

So far, extensive investigations have been conducted on the coherent photoproduction of ρ^0 vector meson at

TABLE I: Ratio of the cross sections for different nuclear neutron configurations, i.e. $\sigma(0n0n)/\sigma(XnXn)$ and $\sigma(0nXn)/\sigma(XnXn)$. Experimental values are from the STAR UPC analysis at $\sqrt{s_{NN}} = 200 \text{ GeV}$, Ref. [25].

Ratio	experiment	theory; $ y_V < 1$	theory - full y_V
$(0n0n)/(XnXn)$	7.1 ± 0.3	6.4	10.1
$(0nXn)/(XnXn)$	3.5 ± 0.2	3.1	3.3

TABLE II: Nuclear cross section in mb for the coherent photoproduction of ρ^0 in $Au + Au$ UPC at $\sqrt{s_{NN}} = 200 \text{ GeV}$. The experimental values of total cross section σ_{exp} are from Ref. [25], $|y_V| < 1$.

Neutron class	σ_{exp}	σ_{th}
$XnXn$	$14.5 \pm 0.7 \pm 1.9$	18.2
$0n0n$	$106 \pm 5 \pm 14^a$	115.6

^abased on the ratio $(0n0n)/(XnXn)$

midrapidity. These experimental studies involved ultraperipheral collisions of Au+Au at RHIC, exploring three distinct center-of-mass energies per nucleon pair: $\sqrt{s_{NN}} = 62.4 \text{ GeV}$ [23], 130 GeV [24], and 200 GeV [25, 26]. Furthermore, the ALICE experiment at the LHC also examined this reaction in lead-lead UPC at a nucleon-nucleon center-of-mass energy of $\sqrt{s_{NN}} = 2.76 \text{ TeV}$ [27] and 5.02 TeV [28].

The STAR experiment has derived $d\sigma/dy_V$ cross section by scaling the mutual excitation ($XnXn$) results due to the poorly known efficiency of the topology trigger. This extrapolation relies on two experimentally measured ratios from the topology sample. The compilation of theoretical results (for two rapidity intervals) with the experimental result is presented in Table I. We start with the ratio of cross sections for different categories for $\sqrt{s_{NN}} = 200 \text{ GeV}$ (STAR), see Table I. The first ratio strongly depends on the range of rapidity. In Table II we show the corresponding cross section in mb . Our model calculation almost reproduces the experimental data.

In Table III we show the cross section for the full rapidity range. The experimental data were obtained by extrapolation from the measured region [25]. In each of the analyzed kinematical configurations, our simple model systematically overestimates the experimental values. Therefore, a more reasonable approach is to analyze the ratios of the results.

Finally in Table IV we show results for the ALICE experiment [28] at the LHC with the collision energy $\sqrt{s_{NN}} = 5.02 \text{ TeV}$. In contrast to RHIC, the present version of the used model gives cross sections which are $\sim 25 \%$ too small. This is caused by too simple parametrization of $\frac{d\sigma(\gamma p \rightarrow \rho^0 p)}{dt} \Big|_{t=0}$ (see Eq. (16)). In the last two columns, we show experimental and theoretical ratios for a given

TABLE III: Nuclear cross section in mb for the coherent photoproduction of ρ^0 in $Au + Au$ UPC at $\sqrt{s_{NN}} = 200$ GeV. The experimental value of total cross section σ_{exp} is taken from Ref. [25], for the full rapidity range.

Neutron class	σ_{exp}	σ_{th}
$XnXn$	$31.9 \pm 1.5 \pm 4.5$	39.3
$Xn0n + 0nXn$	$105 \pm 5 \pm 15$	130.6
$0n0n$	$391 \pm 18 \pm 55$	422.3
no forward neutron selection	$530 \pm 19 \pm 57$	592.1

TABLE IV: Nuclear cross section $d\sigma/dy$ in mb for the coherent photoproduction of ρ^0 in $Pb + Pb$ UPC at $\sqrt{s_{NN}} = 5.02$ TeV. The experimental cross section is provided for different rapidity ranges, Ref. [28].

Neutron class	exp.	theory	r_{exp}^c [%]	$r_{theo.}^c$ [%]
$XnXn$				
$ y < 0.2$	$24.4 \pm 1.3^{+3.4}_{-2.9}$	17.92	4.54	4.39
$0.2 < y < 0.45$	$24.5 \pm 1.2^{+3.4}_{-3.0}$	21.5	4.55	4.42
$0.45 < y < 0.8$	$25.6 \pm 1.3^{+3.5}_{-3.1}$	20.5	4.68	4.49
$Xn0n + 0nXn$				
$ y < 0.2$	$90.2 \pm 1.9^{+10.5}_{-9.5}$	58.2	16.80	14.25
$0.2 < y < 0.45$	$87.7 \pm 1.8^{+10.2}_{-9.3}$	79.6	16.28	14.31
$0.45 < y < 0.8$	$89.9 \pm 2.0^{+10.4}_{-9.5}$	76.2	16.44	14.51
$0n0n$				
$ y < 0.2$	$431.1 \pm 4.0^{+36.8}_{-33.6}$	332.3	80.28	81.39
$0.2 < y < 0.45$	$433.8 \pm 3.8^{+37.0}_{-33.8}$	395.1	80.54	81.25
$0.45 < y < 0.8$	$436.7 \pm 4.2^{+37.3}_{-34.0}$	369.5	79.84	80.98
no forward neutron selection				
$ y < 0.2$	$537.0 \pm 4.6^{+46.1}_{-42.0}$	408.3		
$0.2 < y < 0.45$	$538.6 \pm 4.4^{+46.2}_{-42.1}$	486.3		
$0.45 < y < 0.8$	$547.0 \pm 4.9^{+46.9}_{-42.8}$	456.3		

category defined as:

$$r_c = \frac{d\sigma^c/dy}{\sum_{i=1}^4 d\sigma^i/dy}. \quad (17)$$

The denominator is the sum of contributions from all categories. The "experimental" ratios were obtained from the ALICE data [28]. The partial probabilities for a given neutron category agree with the experimental data for different ranges of rapidity.

Having shown that our approach correctly reproduces fractions of cross sections for a particular neutron category, we can proceed to the case of interest, that is emission of neutrons associated with the $\gamma\gamma \rightarrow \gamma\gamma$ scattering.

C. Neutron emission and light by light scattering

Compared to the experimental and theoretical analysis of vector meson photoproduction associated with neutron emission, such an analysis was not done for LbL

TABLE V: Cross section in nb for light by light scattering in $Pb + Pb$ UPC and different neutron categories. Here $\sqrt{s_{NN}} = 5.36$ TeV corresponding to the ongoing ATLAS analysis.

	σ_{total}	$0n0n$	$XnXn$	$Xn0n + 0nXn$
cross section [nb]	81.886	61.679	4.261	15.963
percent of σ_{total} [%]		75.30	5.20	9.50

scattering. We start by calculating the cross section for different neutron classes and photons in the ATLAS acceptance region: $y_1, y_2 \in (-2.4, 2.4)$ and $p_{t,\gamma} > 2.5$ GeV at the future collision energy $\sqrt{s_{NN}} = 5.36$ TeV. We use the same model, which was discussed in detail, Ref. [12]. and gives relatively good agreement with the experiment. Moving to the main issue of the study, in Tab. V we show a summary of the ratios for the given neutron categories. The cross section for the $0n0n$ category is the biggest and constitutes 75 % of the total fiducial cross section. The cross section for one-side neutron emission constitutes $9.75 \% + 9.75 \% = 19.5 \%$ and the cross section for both side emission is only 5.2 %. These numbers can be compared with similar fractions of neutron classes for ρ^0 production in UPC (see the previous subsection). In general, the fractions in Tables IV and V are similar but not identical.

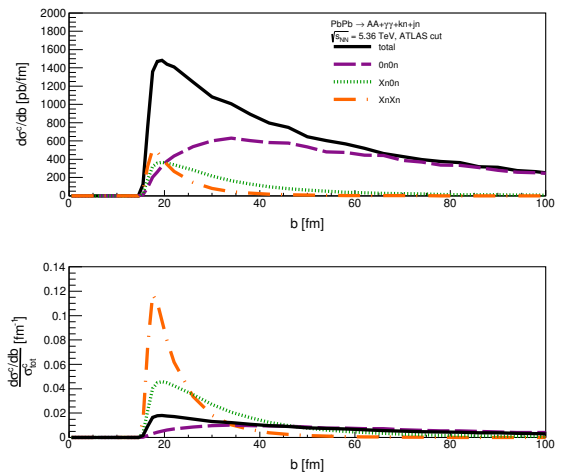


FIG. 2: Impact parameter distribution for: total cross section (solid line), $0n0n$ (dashed line), $Xn0n$ (dotted line) and $XnXn$ (dash-dotted line).

The numbers in Table V can be better understood by inspecting Fig. 2 where the dependence of the cross section on impact parameter is shown.

We show the cross section for different categories. While the $0n0n$ category is related to the broad range of impact parameter, the emission from both nuclei happens at small impact parameters, close to the surface of nuclei ($b \sim 2R_A$). The fluctuations visible in the figure are due to the Monte Carlo method used in our calculation. The distribution in b is rather theoretical and cannot be mea-

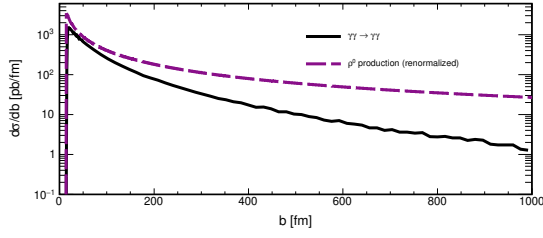


FIG. 3: Impact parameter distribution for ρ^0 production ($\sqrt{s_{NN}} = 5.02$ TeV, $|y| < 1$) and for $\gamma\gamma \rightarrow \gamma\gamma$ ($\sqrt{s_{NN}} = 5.36$ TeV, $|y| < 2.4$, $p_t > 2.5$ GeV). The distribution for ρ^0 production is arbitrarily renormalized.

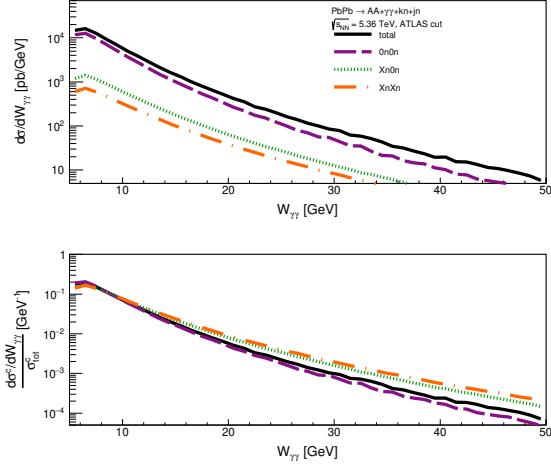


FIG. 4: Diphoton mass distribution of cross section for: total cross section (solid line), and $0n0n$ (dashed line), $Xn0n$ (dotted line) and $XnXn$ (dash-dotted line) categories.

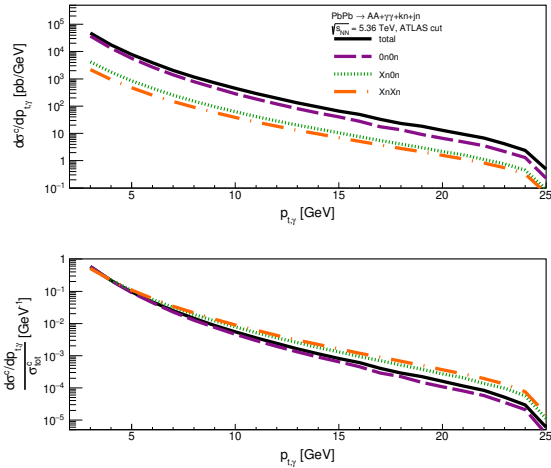


FIG. 5: Transverse momentum distribution for: total cross section (solid line), and $0n0n$ (dashed line), $Xn0n$ (dotted line) and $XnXn$ (dash-dotted line) categories.

sured. The percentage of $0n0n$, $Xn0n + 0nXn$ categories here is smaller than for ρ^0 production (see Table IV). This is associated with relatively larger impact parameters in the ρ^0 production than for the $\gamma\gamma \rightarrow \gamma\gamma$ scattering (see Fig. 3). The distribution for ρ^0 was renormalized arbitrarily in order to compare shapes of distributions.

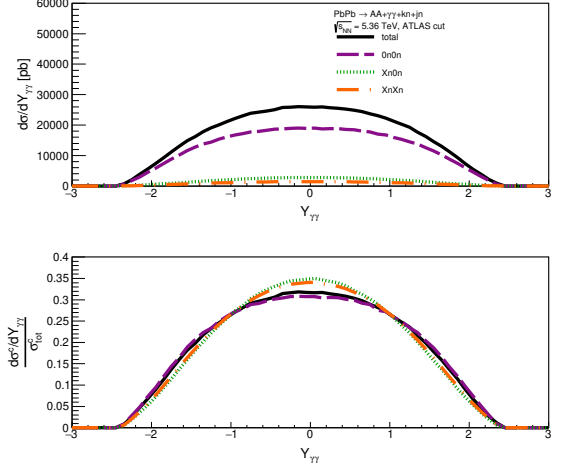


FIG. 6: Rapidity distribution of cross section for: total cross section (solid line), and $0n0n$ (dashed line), $Xn0n$ (dotted line) and $XnXn$ (dash-dotted line) categories.

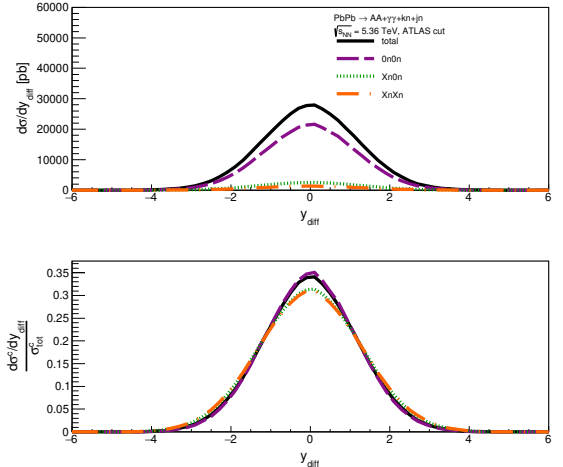


FIG. 7: Rapidity difference distribution of cross section for: total cross section (solid line), and $0n0n$ (dashed line), $Xn0n$ (dotted line) and $XnXn$ (dash-dotted line) categories.

For example, in the following we shall show distributions in possible to measure observables. In Fig.4 we show the distribution in diphoton invariant mass. Taking into consideration only relative contribution, the shape of the distribution weakly depends on the configuration under consideration. Naturally, the largest contribution to the

total cross section comes from the situation when no neutron is emitted from any nucleus.

In Fig.5, Fig.6, Fig.7 we show respectively distributions in photon transverse momentum, diphoton rapidity and distribution in $y_{diff} = y_1 - y_2$. In all cases in the upper panels, we show absolutely normalized cross sections and in the lower panels the distributions normalized to unity in order to compare the shape of the distributions for different neutron classes. By careful inspection of the lower panels we see that the shapes of different observables depend on categorization of neutron emissions.

IV. SUMMARY AND CONCLUSIONS

In the present paper we have discussed in detail the production of neutrons associated with $\gamma\gamma \rightarrow \gamma\gamma$ scattering in UPC of $^{208}\text{Pb} + ^{208}\text{Pb}$. We have presented the cross sections for different neutron categories and for photon cuts of the respective recent ATLAS experiment. We have also shown fractions of cross sections for different neutron categories and compared them with similar fractions for ρ^0 meson production in UPC. In general, the fractions for both cases (ρ^0 production and $\gamma\gamma \rightarrow \gamma\gamma$) are similar, but not identical.

We have presented the impact parameter dependence of the probability of a given neutron category ($0n0n$, $0nXn + Xn0n$, $XnXn$). We have also briefly discussed the impact of a recent measurement of the ESR collaboration at GSI/FAIR Darmstadt of the probability of neutron emissions at low excitation energies close to neutron separation energy. We have found that there are rather small corrections to the cross section at the % level.

We have calculated several differential distributions in photon variables (rapidity, transverse momentum, diphoton invariant mass and rapidity difference) separately for different neutron categories. We have demonstrated how the shape of the distribution depends on the choice of neutron categories.

We hope our predictions will be confronted by the ATLAS experimental results in the near future. In the present paper, we have considered the dominant coherent contribution, called sometimes elastic-elastic or double elastic. The potential contribution of inelastic processes (photon couples to nucleons) discussed by us recently [13] requires a special attention which goes beyond the scope of the present letter. The deviation of experimental numbers from our predictions on fractions of topological cross sections may signal a participation of inelastic contributions [13]. We suggest that the ATLAS collaboration could measure the fractions of cross sections also for larger transverse momenta of diphotons $p_{t,\gamma\gamma}$ or larger acoplanarities than used for selection of the $\gamma\gamma \rightarrow \gamma\gamma$ scattering. This would provide interesting information on the background contribution which is not well understood so far in our opinion.

Acknowledgment

We are indebted to Michał Ciemala for pointing to us the recent GSI result [22] on the probability of the neutron emission at low excitation energies and Iwona Grabowska-Bold for a discussion of the ATLAS experiment and plans of the ATLAS collaborations for the future.

-
- [1] M. Aaboud and others (ATLAS Collaboration). Evidence for light-by-light scattering in heavy-ion collisions with the ATLAS detector at the LHC. *Nature Phys.*, 13: 852–858, 2017. doi: 10.1038/nphys4208.
 - [2] A. M. Sirunyan and others (CMS Collaboration). Evidence for light-by-light scattering and searches for axion-like particles in ultraperipheral PbPb collisions at $\sqrt{s_{NN}} = 5.02$ TeV. *Phys. Lett. B*, 797:134826, 2019. doi: 10.1016/j.physletb.2019.134826.
 - [3] G. Aad and others (ATLAS Collaboration). Observation of light-by-light scattering in ultraperipheral Pb+Pb collisions with the ATLAS detector. *Phys. Rev. Lett.*, 123(5):052001, 2019. doi: 10.1103/PhysRevLett.123.052001.
 - [4] G. Aad and others (ATLAS Collaboration). Measurement of light-by-light scattering and search for axion-like particles with 2.2 nb⁻¹ of Pb+Pb data with the ATLAS detector. *JHEP*, 03:243, 2021. doi: 10.1007/JHEP11(2021)050. [Erratum: JHEP 11, 050 (2021)].
 - [5] A. Abreu et al (CMS Collaboration). Measurement of light-by-light scattering and the Breit–Wheeler process, and search for axion-like particles in ultraperipheral PbPb collisions at $\sqrt{s_{NN}} = 5.02$ TeV. *CERN Document Server*, CMS-PAS-HIN-21-015, Apr 2024.
 - [6] M. Khusek-Gawenda, P. Lebiedowicz, and A. Szczurek. Light-by-light scattering in ultraperipheral Pb-Pb collisions at energies available at the CERN Large Hadron Collider. *Phys. Rev. C*, 93:044907, Apr 2016. doi: 10.1103/PhysRevC.93.044907.
 - [7] M. Khusek-Gawenda, W. Schäfer, and A. Szczurek. Two-gluon exchange contribution to elastic $\gamma\gamma \rightarrow \gamma\gamma$ scattering and production of two-photons in ultraperipheral ultrarelativistic heavy ion and proton-proton collisions. *Phys. Lett. B*, 761:399–407, 2016. doi: 10.1016/j.physletb.2016.08.059.
 - [8] P. Lebiedowicz and A. Szczurek. The role of meson exchanges in light-by-light scattering. *Phys. Lett. B*, 772: 330–335, 2017. doi: 10.1016/j.physletb.2017.06.060.
 - [9] M. Khusek-Gawenda, R. McNulty, R. Schicker, and A. Szczurek. Light-by-light scattering in ultraperipheral heavy-ion collisions at low diphoton masses. *Phys. Rev. D*, 99(9):093013, 2019. doi: 10.1103/PhysRevD.99.093013.
 - [10] C. Loizides, W. Riegler, and others (ALICE Collaboration). Letter of Intent: A Forward Calorimeter (FoCal) in the ALICE experiment. *CERN Document Server*, CERN-LHCC-2020-009 ; LHCC-I-036, Jun 2020.

- [11] L. Musa, W. Riegler, and others (ALICE Collaboration). Letter of intent for ALICE 3: A next-generation heavy-ion experiment at the LHC. *CERN Document Server*, CERN-LHCC-2022-009, LHCC-I-038, Mar 2022.
- [12] P. Jucha, M. Klusek-Gawenda, and A. Szczurek. Light-by-light scattering in ultraperipheral collisions of heavy ions at two future detectors. *Phys. Rev. D*, 109:014004, Jan 2024. doi: 10.1103/PhysRevD.109.014004.
- [13] M. Klusek-Gawenda, V. P. Gonçalves, and A. Szczurek. Light-by-light scattering in ultraperipheral heavy ion collisions: Estimating inelastic contributions. *Physics Letters B*, 867:139614, 2025. ISSN 0370-2693. doi: <https://doi.org/10.1016/j.physletb.2025.139614>.
- [14] A. Baltz, S. R. Klein, and Nystrand J. Coherent Vector-Meson Photoproduction with Nuclear Breakup in Relativistic Heavy-Ion Collisions. *Phys. Rev. Lett.*, 89(1): 012301, 2002. doi: 10.1103/PhysRevC.89.012301.
- [15] A. Baltz, Y. Gorbunov, S. R. Klein, and Nystrand J. Two-photon interactions with nuclear breakup in relativistic heavy ion collision. *Phys. Rev. C*, 80(4):044902, 2009. doi: 10.1103/PhysRevC.80.044902.
- [16] I. A. Pshenichnov. Multiphoton exchanges in peripheral heavy ion collisions. *Physics of Particles and Nuclei*, 42: 215–250, 2011. doi: 10.1134/S1063779611020067.
- [17] M. Klusek-Gawenda, M. Ciemala, W. Schäfer, and A. Szczurek. Electromagnetic excitation of nuclei and neutron evaporation in ultrarelativistic ultraperipheral heavy ion collisions. *Phys. Rev. C*, 89(5):054907, 2014. doi: 10.1103/PhysRevC.89.054907.
- [18] S. R. Klein, J. Nystrand, J. Seger, Y. Gorbunov, and J. Butterworth. Starlight: A monte carlo simulation program for ultra-peripheral collisions of relativistic ions. *Computer Physics Communications*, 212:258–268, 2017. ISSN 0010-4655. doi: <https://doi.org/10.1016/j.cpc.2016.10.016>.
- [19] M. Broz, J.G. Contreras and J.D. Tapia Takaki. A generator of forward neutrons for ultra-peripheral collisions: n_o^n . *Comp. Phys. Commun.*, 253:107181, 2020. doi: 10.1016/j.cpc.2020.107181.
- [20] E. Kryshen, M. Strikman, and M. Zhalov. Photoproduction of J/ψ with neutron tagging in ultraperipheral collisions at RHIC and at the LHC. *Phys. Rev. C*, 108(2):024904, 2023. doi: 10.1103/PhysRevC.108.024904.
- [21] P. Jucha, M. Klusek-Gawenda, A. Szczurek, M. Ciemala, and K. Mazurek. Neutron emission from the photon-induced reactions in ultraperipheral ultrarelativistic heavy-ion collisions. *Phys. Rev. C*, 111:034901, Mar 2025. doi: 10.1103/PhysRevC.111.034901.
- [22] I. Gheorghe et al. Photoneutron cross section measurements on ^{208}Pb in the giant dipole resonance region. *Phys. Rev. C*, 110:014619, Jul 2024. doi: 10.1103/PhysRevC.110.014619.
- [23] G. Agakishiev et al. ρ^0 Photoproduction in AuAu Collisions at $\sqrt{s_{NN}}=62.4$ GeV with STAR. *Phys. Rev. C*, 85: 014910, 2012. doi: 10.1103/PhysRevC.85.014910.
- [24] C. Adler et al. Coherent ρ^0 production in ultraperipheral heavy ion collisions. *Phys. Rev. Lett.*, 89:272302, 2002. doi: 10.1103/PhysRevLett.89.272302.
- [25] B. I. Abelev et al. ρ^0 photoproduction in ultraperipheral relativistic heavy ion collisions at $\sqrt{s_{NN}} = 200$ GeV. *Phys. Rev. C*, 77:034910, 2008. doi: 10.1103/PhysRevC.77.034910.
- [26] L. Adamczyk et al. Coherent diffractive photoproduction of ρ^0 mesons on gold nuclei at 200 GeV/nucleon-pair at the Relativistic Heavy Ion Collider. *Phys. Rev. C*, 96(5): 054904, 2017. doi: 10.1103/PhysRevC.96.054904.
- [27] J. Adam et al. Coherent ρ^0 photoproduction in ultraperipheral Pb-Pb collisions at $\sqrt{s_{NN}} = 2.76$ TeV. *JHEP*, 09:095, 2015. doi: 10.1007/JHEP09(2015)095.
- [28] S. Acharya et al. Coherent photoproduction of ρ^0 vector mesons in ultra-peripheral Pb-Pb collisions at $\sqrt{s_{NN}} = 5.02$ TeV. *JHEP*, 06:035, 2020. doi: 10.1007/JHEP06(2020)035.